Available online at www.sciencedirect.com

SCIENCE DIRECT

Cement and Concrete Research 35 (2005) 2033 – 2040

Cement and Concrete Research

Magnetic resonance studies of cement based materials in inhomogeneous magnetic fields

Joanna Boguszynska [b], Marc C.A. Brown [c], Peter J. McDonald [a,*], Jonathan Mitchell [a], Mike Mulheron [d], Jadwiga Tritt-Goc [b], Dimitris A. Verganelakis [e]

[a] School of Electronics and Physical Sciences, University of Surrey, Surrey, GU2 7XH, United Kingdom
[b] Institute of Molecular Physics, Polish Academy of Sciences, Smoluchowskiego 17, Poznan, Poland
[c] School of Physical Sciences, University of Kent, Canterbury, Kent, CT2 7NR, United Kingdom
[d] School of Engineering, University of Surrey, Surrey, GU2 7XH, United Kingdom
[e] Department of Chemical Engineering, University of Cambridge, Cambridge, CB2 3RA, United Kingdom

Received 13 July 2004; accepted 22 June 2005

Abstract

Single-sided magnets give hope that Nuclear Magnetic Resonance (NMR) might in future be used for in situ characterisation of hydration and water transport in the surface layers of concrete slabs. Towards that end, a portable NMR-MOUSE (MObile Universal Surface Explorer) has been used to follow the hydration of gypsum based plaster, a Portland cement paste and concrete mortar. The results compare favourably to those obtained using a standard laboratory bench-top spectrometer. Further, stray field imaging (STRAFI) based methods have been used with embedded NMR detector coils to study water transport across a mortar/topping interface. The measured signal amplitudes are found to correlate with varying sample conditions.

Keywords: NMR; Curing; Pore size distribution; Transport properties; Cement paste

1. Introduction

Structural concrete slabs are commonly used in large-scale construction projects. They are often covered with a cementitious screed or topping, typically 10–50 mm thick in order to improve the in-service performance of the slab, to provide the required tolerance levels for flatness and to improve the aesthetics of the structure. During the construction phase, there are considerable time pressures to complete the application of the topping as quickly as possible after the lower layer has sufficiently matured. Subsequently, to prevent blistering and delamination, it is important to ensure that water does not build up at the concrete/topping interface [1]. Two problems therefore exist: how to determine if the concrete in the slab is sufficiently dry to allow finishing, and how to detect water accumulation at the concrete/topping interface. As a result, there is a need for practical methods to assess moisture condition in concrete slabs. Historically, "rule-of-thumb" drying periods have been successful in determining the minimum drying time required for ordinary Portland cement (OPC) based concrete before a topping could be applied. However, modern blended cements with improved chemical admixtures have led to the formation of low permeability concretes that can take considerably longer to dry. Nuclear Magnetic Resonance (NMR) may provide a non-destructive measurement solution to the problem.

NMR measurements conducted on ^{1}H (water) in homogeneous magnetic fields have been shown to provide information on hydration, drying and water transport in small samples of cements and mortars under laboratory conditions [2–5]. The NMR signal from hydrated OPC normally comprises of three principal components that exhibit different relaxation times, one each for chemically

* Corresponding author.
E-mail address: p.mcdonald@surrey.ac.uk (P.J. McDonald).

0008-8846/$ - see front matter © 2005 Elsevier Ltd. All rights reserved.
doi:10.1016/j.cemconres.2005.06.012

combined water, and water in gel and capillary pores [2]. Others have suggested more components that offer further refinement to this classification[6,7]. Their relative amplitudes reflect the volume of water in each environment, whilst the relaxation times are related to the degree of confinement of the water molecules. In this work, we extend the use of NMR to larger samples measured in inhomogeneous magnetic fields using (i) a mobile universal surface explorer (the so-called NMR-MOUSE ® [8,9]) and (ii) detector coils embedded in a sample and placed in the fringe field of a large, super-conducting magnet.

The MOUSE is a handheld sensor for measuring the NMR response from surface layers (0–7 mm) of samples. It has been shown to be suitable for estimating the porosity of historic building materials [10]. We use it to observe the hydration and subsequent drying of gypsum based finishing plaster [11], OPC [12], and pre-prepared concrete mortar. The results are compared to those obtained from a bench-top Maran Ultra NMR spectrometer manufactured by Resonance Instruments Ltd [13]. The three samples are chosen because they are characterised by increasing levels of structural heterogeneity and paramagnetic ions. Local magnetic field gradients necessarily occur in heterogeneous and porous media due to local variations in magnetic susceptibility. Water diffusion through these gradients is an additional relaxation mechanism that complicates data analysis. The problem is exacerbated by paramagnetic impurities.

Embedded NMR coils can be used to measure the response from deeper layers (0–75 mm). We place coils at different depths in mortar/topping samples to monitor the water distribution in the vicinity of the interface between the two materials. By independently exposing the mortar and topping to moisture, the transport of water across the interface is observed under simulated environmental conditions. Although the method is not necessarily viable in the working environment (a variant has been suggested for studying moisture in road surfaces [14]), the method may be suited to studies of concrete toppings in the laboratory that could verify improved “rule-of-thumb” drying periods.

2. Materials

The first sample used for MOUSE analysis is a gypsum based plaster with water-to-plaster ratio of 0.40 by volume. Once mixed with water, the plaster forms a uniform paste with minimal paramagnetic ion content. Of the three, it is the most amenable to NMR analysis. The second is OPC with a water-to-cement (w/c) ratio of 0.45. Portland cement contains paramagnetic ions, although the paste is uniform and free of aggregates. The third sample is a pre-prepared concrete mortar (containing OPC and fine aggregate particles <2 mm diameter) mixed with 10% water by volume (corresponding to a w/c ratio of 0.45). The aggregate creates further structural inhomogeneity. The plaster, cement and concrete samples were made by thoroughly mixing the dry ingredients and water by hand. The samples were cured sealed in plastic weigh boats $50 \times 50 \times 40$ mm^3. The same mixes were used for samples analysed on the standard bench-top spectrometer: these were sealed in regular 10 mm test tubes.

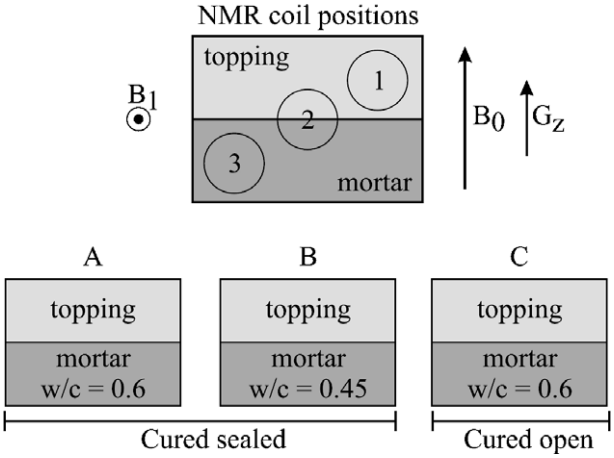

Fig. 1. Schematic of embedded coil stray field NMR samples. (Upper image) three NMR coils were placed in the sample to measure the topping, interface and mortar. The stray field measurement recorded one-dimensional profiles vertically across the coils, parallel to the magnetic field (B_0) and gradient (G_z) and normal to the sensor field (B_1). (Lower image) three samples were made (A–C) using different mortar and topping layers. Samples A and B were cured sealed, whereas sample C was cured open.

The mortar used for the surface interface measurements was a mix of sand and OPC in the ratio of 4 : 1 by mass, with a w/c ratio of either 0.60 (samples A and C) or 0.45 (sample B) by mass. The cementitious topping was a commercial self- levelling compound, a blend of cements and organic binders. Following the manufacturers instructions, 4 parts of the topping powder were mixed with 1 part water by volume. All three samples had identical toppings. Die-cast aluminium boxes ($188 \times 119 \times 78$ mm^3) were used to mould the mortar and support three NMR coils. The positions of the NMR coils can be seen in the upper part of Fig. 1. The pour of mortar half-filled the boxes and covered one and a half coils. This was left to cure for 7 days. A pour of topping was then applied to completely fill the boxes and the remaining coils. Samples A and B were cured sealed whereas sample C was left open to the environment during cure. The details of the three individual samples have been schematically summarised in the lower part of Fig. 1.

3. Experimentation

The MOUSE was tuned to a ^{1}H resonant frequency of 20 MHz so that the signal originated from a small volume just above the base of the weigh boat. In order to observe the spin–spin relaxation time (T_2) in the inhomogeneous magnetic field, echo trains were recorded using an α_x-(τ-$2\alpha_y$-τ-echo)$_n$ pulse sequence, where α is a radio-frequency pulse of nominal spin flip angle 90° (equal to 2.6 μs) with

relative quadrature phase x or y, and $\tau = 30$ μs. In each scan, 1500 echoes were recorded; 640 scans were acquired with a repeat delay of 1 s to provide an acceptable signal-to-noise ratio. The samples were measured hourly for 24 h after mixing and then twice daily for 7 days with a final measurement after 28 days. The measured T_2 decays were then inverted [15] using Resonance Instruments Ltd. Windows Distributed Exponential Function (WinDXP) to provide a distribution of relaxation times that could be related to the water confined in the pore structures [5]. NMR data obtained from cementitious samples often has a low signal-to-noise ratio. The instability of inversion functions when analysing noisy data has been discussed elsewhere [16]. Accordingly, the relaxation data were also analysed by single exponential 'stretch' fits [17] using Eq. (1), where M is the signal intensity, t is the experimental time, and β defines the shape of the relaxation curve relative to a perfect exponential decay ($\beta = 1$) and is indicative of the distribution of T_2 values.

$$M(t) = M(0)\exp\left[-\left(\frac{t}{T_2}\right)^{\beta}\right]. \quad (1)$$

The Maran Ultra spectrometer is a desktop NMR device based on a homogeneous 0.55 T permanent magnet, having a corresponding ^{1}H proton resonant frequency of 23 MHz. Echo trains were recorded using the same parameters as with the MOUSE measurements, and again the relaxation data were inverted using WinDXP.

The embedded coil measurements were conducted in the fringe field of a 0.7 T, 20 cm horizontal bore superconducting magnet, equipped with a Resonance Instruments Ltd. Maran DRX digital spectrometer. The coils, each approximately 20 mm in diameter, were tuned to 2.6 MHz, corresponding to a position 100 mm from the end of the magnet where the fringe field and gradient were 0.06 T and 0.5 T/m, respectively. The samples were placed in the fringe field so that the normal to the cement/topping interface was parallel to the field (B_0) and gradient (G_z) direction; see Fig. 1. Signals were obtained from each coil using broad-band excitation pulses which spanned the full frequency spectrum of the enclosed material in one scan. The α_x-(τ-2α_y-τ-echo)$_n$ pulse sequence was used with $\alpha = 2$ μs, corresponding to an 18° nominal spin flip angle. In a magnetic field gradient the width of the selected volume-slice is inversely proportional to the length of the excitation pulse. The flip angle was chosen to complement the diameter of the embedded coils. Eight echoes were captured in each scan, with $\tau = 100$ μs. The echoes were Fourier Transformed and co-added with the intention to provide profiles across the measurement zone of the coil with high spatial resolution, particularly at the interface. Unfortunately the resultant profiles were not of sufficient quality to allow meaningful analysis of this kind. The three one-dimensional profiles were instead integrated to provide a total water signal for four regions in each sample: coil 1 (topping), the upper half of coil 2 (interface — topping), the lower half of coil 2 (interface — mortar), and coil 3 (mortar).

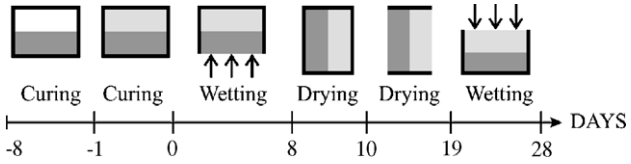

Fig. 2. Experimental timeline showing the process by which the mortar (dark grey) and the topping (light grey) were cured and then exposed to water (indicated by arrows at surfaces). NMR measurements began on day zero. The thick black lines around the samples represent the aluminium box and box lids used to seal/expose the sample. (Sample C was cured open at the top).

The samples were sufficiently dry to allow the boxes to be appropriately positioned in the stray field and measured 24 h after applying the topping layer. A time-line of the subsequent experimental procedure can be seen in Fig. 2. Measurements started at day zero when the boxes were opened, just before the base of each sample was exposed to water by standing on a wet sponge. Water exposure from the base continued for 7 days. From day 7 the samples were allowed to dry, but to prevent over-rapid drying at the start the boxes were kept closed for the next 3 days. On day 10 the samples were opened both at the top and bottom and allowed to dry for a further 9 days. Finally the top of each sample was exposed to water for 9 days, with the bottom once again sealed. NMR measurements were taken regularly throughout the 28-day experiment. The samples were weighed at the same time as the NMR measurement to provide an indication of hydration and water absorption/loss.

4. Results

4.1. MOUSE studies

Exemplar results from the initial hydration studies of cementitious materials using the MOUSE and Maran systems can be seen in Fig. 3. The areas under the relaxation time distributions have been normalised to the results from day 1.

For the plaster, the relaxation time distributions calculated from the experimental results from the MOUSE and Maran both show two components that evolve similarly with time. One peak is centred at 0.01 s and is attributed to water in the larger pores. A second much smaller peak is observed centred between 0.1 and 1.0 ms. This is attributed to the water in the fine pores of the hydrated calcium sulphate, analogous to the calcium silicate hydrate gel pores of OPC. Using the fast exchange relaxation theory [18,19] and an estimate of surface relaxivity of $T_2^S = 10$ μs [2], the former corresponds to pore sizes of ~10 nm and the latter to pore sizes of 0.3 μm. The intensity of both peaks decreases whilst the width increases with time. The most significant difference is in the Maran results on day 7 where the main relaxation time peak intensity is less than for the corre-

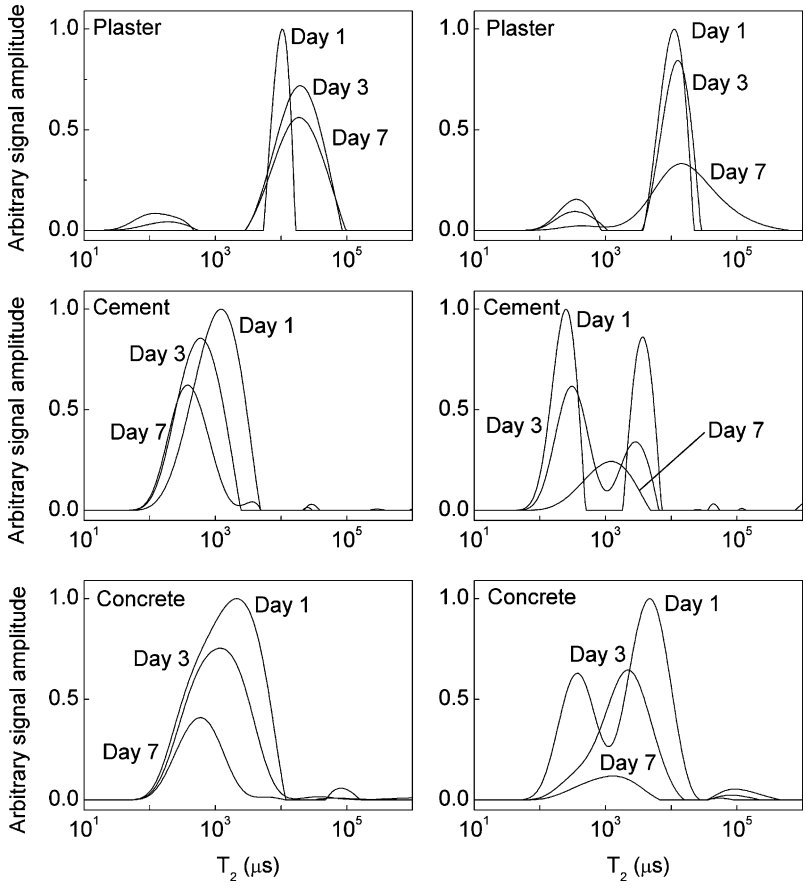

Fig. 3. Relaxation time distributions from MOUSE (left) and Maran (right) measurements of hydrating samples. Graphs show data recorded on three occasions over one week as the samples were cured sealed.

sponding MOUSE data, but the peak is broader possibly suggesting a more sensitive measurement. An alternative analysis is based on the stretched exponential fit of Eq. (1). From this analysis, the β terms (see Table 1) were similar for both spectrometers, suggesting the shape of the T_2 decays varied consistently over the course of the experiment. In both analyses the dominant T_2 value in the plaster increases with time. Gypsum plasters are known to decay in the long-term presence of water and the increased relaxation time almost certainly reflects the concomitant changes in the pore structure.

The cement samples are considered next. Initially the relaxation time distributions from the Maran data clearly show two distinct peaks centred at 0.2 and 3 ms (see Fig. 3), corresponding to the evolving gel and capillary pores, respectively. As the sample cured, the two peaks merged into a single broad peak. It is believed that the mathematical inversion function was unable to resolve two peaks given the poor signal-to-noise ratio of the data. The relaxation time distributions from the cement measurements using the MOUSE were all of low resolution and only a single, broad relaxation time peak was resolved, corresponding to the average T_2 from the water in all the pores. The peak was seen to decrease in intensity as the hydration process bound the available water into the CSH of the cement paste.

The concrete mortar gave results similar to those from the cement samples, although the total signal amplitude was lower in all measurements due to the reduced water content in the initial mix. Two peaks were distinguishable in the first Maran measurement, but the signal-to-noise rapidly degraded as the hydration progressed, so only an average T_2 peak could

Table 1
Single exponential 'stretch' fits of T_2 relaxation data recorded on the MOUSE and Maran spectrometers from samples during 7 days of hydration

	MOUSE		Maran	
	T_2 (ms)±0.1	β±0.05	T_2 (ms)±0.02	β±0.05
Plaster				
Day 1	8.8	0.93	9.4	0.88
Day 3	14.4	0.82	10.9	0.87
Day 7	17.3	0.79	12.8	0.80
Cement				
Day 1	7.2	1.00	4.5	0.88
Day 3	1.4	0.75	0.6	0.86
Day 7	0.7	0.68	0.4	0.68
Concrete				
Day 1	7.3	1.00	3.3	0.61
Day 3	2.1	0.99	1.0	0.53
Day 7	0.5	0.36	0.3	0.43

be resolved. The stretch fits for all the cement and concrete measurements tell a consistent story (Table 1). Between days 1 and 8, both the β term and the average T_2 decreased, consistent with the evolution of the complex pore structure in OPC. The average T_2 values estimated from the Maran data were half those estimated from the MOUSE data. The complex modulation of echoes recorded in inhomogeneous fields may have resulted in the shorter T_2 components being poorly represented in the MOUSE data. All the cement and concrete mortar samples were re-measured 28 days after mixing, when a further decrease in signal intensity was observed without a variation in β or T_2 compared to day 8, when the samples were opened and exposed to air. This suggested that the volume of evaporable water had decreased without substantial evolution of the pore structure.

As previously mentioned, these samples reflect a progression of increasing structural heterogeneity and paramagnetic impurity concentration in the order gypsum plaster, OPC paste, and concrete. The relaxation analysis reveals the same trend. The T_2 values are known to be dependant on the concentration of paramagnetic ions at the pore solid/liquid interface [20]. These impurities enhance relaxation and give rise to T_2 times that are shorter than may otherwise be expected. From Table 1 (considering the Maran data) it can be seen that the mean relaxation times over the 7 days decrease in the order plaster (~11 ms), cement (~1.8 ms), and concrete (~1.5 ms). Similarly the β values can be taken as an indication of structural complexity and width of the pore size distribution in these samples [21]. $\beta=1$ suggests a narrow distribution of pore sizes; smaller values, a broader distribution. Again considering the Maran data in Table 1, it can be seen that the gypsum plaster – assumed to have the simplest pore structure – has a high β value (0.80–0.88) and a pore size distribution dominated by a single narrow peak: see Fig. 3. By contrast the "complex" concrete has a low β value (0.43–0.61) suggesting a more heterogeneous pore structure. This is corroborated by the pore size distribution measured on day 1 (Fig. 3) that consists of two distinct peaks over a wide range of T_2 values.

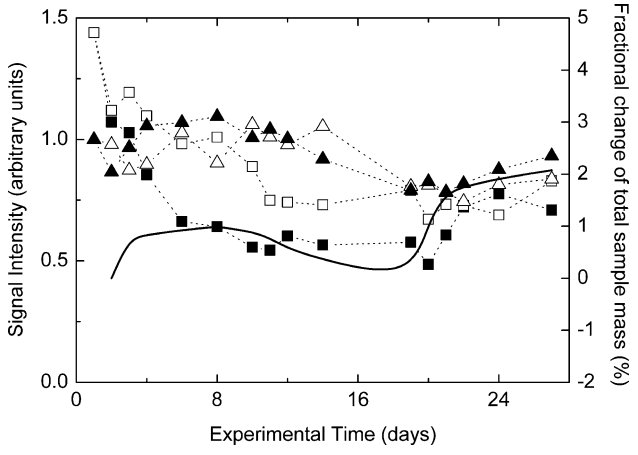

Fig. 4. Variation of integral signal intensities for sample A from the three embedded coils (coil 2 split into upper and lower halves) and the change of total sample mass relative to the mass on day zero as a function of the experiment time. See Fig. 2 for explanation of experimental timeline. The symbols represent coil 1 (topping): filled squares; coil 3 (mortar): filled triangles; coil 2 upper half: open squares; coil 2 lower half: open triangles. The fractional mass change (solid line) is scaled on the right-hand axis.

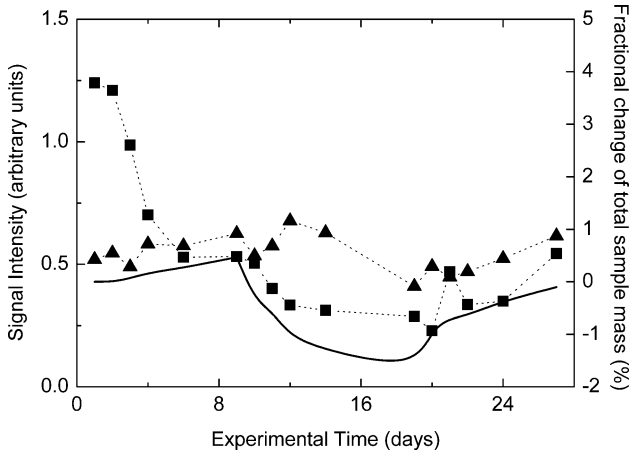

Fig. 5. Variation of integral signal intensities for sample B from the three embedded coils and the change of total sample mass relative to the mass on day zero as a function of the experiment time. See Fig. 2 for explanation of experimental timeline. See Fig. 4 caption for explanation of symbols. The results from the interface coil (coil 2) have been omitted from this graph for clarity.

4.2. Embedded coil studies: initial data

The stray field measurements using embedded NMR coils provide an indication of the variation in mobile water content in the mortar/topping samples over the 28 day experimental cycle shown in Fig. 2. The recorded magnetisation from coils 1 and 3 in samples A, B, and C can be seen in Figs. 4 5 and 6, respectively. The signal from each coil in each sample at all times was normalised relative to the signal from coil 1 in

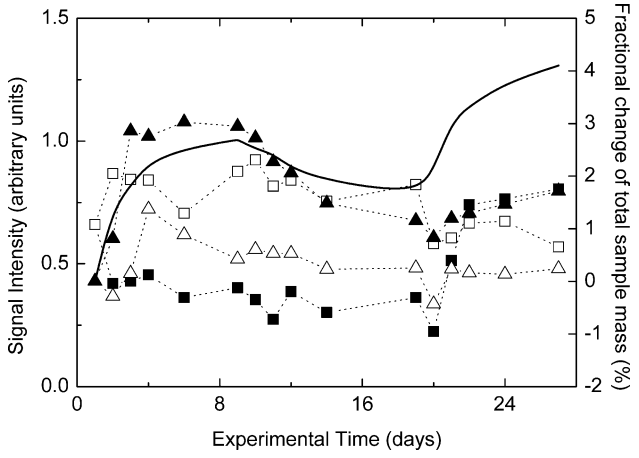

Fig. 6. Variation of integral signal intensities for sample C from the three embedded coils and the change of total sample mass relative to the mass on day zero as a function of the experiment time. See Fig. 2 for explanation of experimental timeline. See Fig. 4 caption for explanation of symbols.

Table 2
Relative initial integrated signal intensities from the coils embedded in the upper (topping) and lower (mortar) regions of the samples, compared to the lower layer signal intensity in sample A

Sample	Upper layer initial signal intensity	Upper layer percentage evaporable water	Lower layer initial signal intensity	Lower layer percentage evaporable water
A	1.44	24.6±1.5	1.00	15.0
B	1.24	21.1±1.3	0.52	9.5
C	0.66	11.3±0.7	0.43	7.7

The percentage evaporable water (gel+capillary) in the lower layer at the start of the measurements was calculated from the original water content of the mix. The percentage evaporable water in the upper layer was estimated from the signal intensities (see text).

sample A at the start (see Table 2). The variation in mass for each sample relative to the initial mass can also be seen in the figures. Initially coil 3 in the lower layer of sample A shows more than twice the magnetisation than the corresponding coil in sample C. These two samples are identical (mortar with w/c ratio=0.6, plus topping) except that sample A was cured sealed, while sample C was cured open. Qualitatively, the result is therefore as expected: sample C dried during curing. Table 2 includes a numerical estimate of the percentage volume of evaporable water calculated for the mortar using the initial quantities and known densities of water, sand (2.6 g/cm^3), and cement (3.15 g/cm^3) together with a "rule-of-thumb" that a mass of water equal to 42% the mass of cement is required to fully hydrate the cement, with 23% going to chemical reactions and 19% going to the gel pores, and that the reacted water undergoes 25.4% shrinkage leading to the creation of the capillary voids [22]. On this basis the mortar in sample A consists of 82.6% solids, 7.3% capillary water, 7.7% gel water, and 2.4% capillary void. Sample C is similar except that the 7.3% capillary water evaporates leaving up to 7.3% additional capillary void. The expected ratio of the initial signal intensities between samples C and A is therefore 7.7/(7.7+7.3)=0.51, a little higher than the experimental value of 0.43. Like sample A, the mortar in sample B was cured sealed but had a lower w/c ratio of 0.45. Accordingly the mortar layer in sample B was calculated to contain 87.9% solids, 1.3% capillary water, 8.2% gel water, and 2.5% capillary voids. The expected ratio of the initial signal intensities between samples B and A is then (8.2+1.3)/(7.7+7.3)=0.63. This is again higher than the experimental value of 0.52, although the two values are still in reasonably good agreement. The fact that both theoretical ratios are consistently high maybe first due to the different relaxation times, and hence different weightings, of gel and capillary water in the NMR measurement that are not considered in this simple analysis, and second to the fact that the samples remain relatively young and may not have reached an equal stage of maturity.

The percentage of evaporable water in the topping layers could not be calculated using the "rule-of-thumb" because neither the precise w/c ratio in the premixed self-levelling compound nor the aggregate was known. It was assumed that the initial signal intensities obtained from the coils in the topping and in the mortar were directly comparable. A mean conversion factor from evaporable water to relative signal intensity was calculated to be 17.0±1.0% water per unit signal, based on the results from the mortar layers. This value is clearly instrument specific. From this average percentage of water in the mortar layers, the percentage of evaporable water in the topping layers was estimated; see Table 2. These values indicate much higher water contents in the toppings than in the mortars. This is not unreasonable since the topping is a wet, free-flowing material when laid which hardens to a dense, impermeable layer that is expected to limit the movement of water in any given time period. For illustrative purposes, an evaporable water content of 24.6% is consistent with a topping formulated with a w/c ratio of 0.65 and a sand-aggregate / cement ratio of 1, together with the assumption that the topping powder had a loose packing factor of 2/3 in the original mix measurement volume (24.7% evaporable water by the "rule-of-thumb"). Of course there are other sample mixes which achieve the same theoretical evaporable water content, although the w/c or aggregate/cement ratios are not always reasonable. The signal intensity from topping B was expected to be the same as the signal intensity from topping A since both layers were cured under identical conditions, and the estimated values are indeed similar. The evaporable water content of topping C was much less (by a factor of 1/2) than in either of the other two toppings. This layer was cured open and so some fraction of the water in the capillary pore network could evaporate into the atmosphere.

4.3. Embedded coil studies: time series data

During the first 8 days of the measurement when the lower side of the samples were exposed to water, the lower coil in sample A shows only a slight overall increase in signal intensity; see Fig. 4. This is consistent with the sample being almost entirely saturated at the outset (2.4% capillary void). This is also true for sample B; see Fig. 5. Immediately upon opening sample A on day 1, we observe a drop in intensity perhaps due to immediate evaporation of excess capillary water and the sample reaching a new dynamic equilibrium. The signal from the lower coil in sample C (Fig. 6) more than doubles over the first 2 days and attains a value very similar to sample A, suggesting that the capillary voids fill with water. Between days 8 and 19 the samples were dried. The signal from coil 3 in sample A decreases by 30% over this period, consistent with the loss of water from the capillary pores. Both the size of the decrease and the gradient of the curve suggest that the capillary pores are not empty by day 19. Sample B also shows a decrease during this period, as does sample C. Finally the top side of the samples were exposed to water. The signal

from each of the lower coils increases but not as rapidly, for instance, as when the lower side of the samples was wet. This is consistent with the impermeable topping material affording some degree of protection to the lower layer against water ingress.

We now turn our attention to the toppings. In all the samples, but especially A and B, there is a very rapid drop in signal intensity from the coils in the toppings during the first day or so. This is explained by ongoing curing. Sample C shows only half the signal of A and B and a smaller initial decrease. This is because the topping was able to dry during the one day of open cure leading up to the first measurement. There is no evidence that the topping absorbs moisture from the lower mortar during the first 8 days. In sample B there is evidence of drying of the toppings from day 10 when the samples were opened, although this is not seen in samples A and C. One possibility is that excess water in the topping of sample B could not invade the (presumably) more closed capillary pore structure of the lower layer, compared to A and C in the preceding few days. All three topping layers show a signal increase during the final stage of wetting from above.

The percentage change in mass of each sample as a function of time is at most 5%, an order of magnitude less than the percentage changes in signal intensities which vary by as much as 50%. The mass change comes about from changes in water content compared to the total mass, whereas the NMR signal changes with the evaporable water content and mobility. NMR is therefore fundamentally more sensitive than conventional gravimetric methods in following the hydration process. Nonetheless, the mass changes broadly follow the net change in NMR signal intensity from coils 1 and 3 except when the NMR measurement reveals changes in the water mobility but not content, e.g. during the first day or so of topping cure.

The signal from the interface coil, coil 2, in each sample is considerably noisier than that from coils 1 and 3, in part because it has been divided into an upper and lower portion. Still, these divided signals generally follow the signals from the corresponding coils in the upper and lower layers, to which they have been normalised on day zero, albeit often with a short time lag, perhaps reflecting the more deeply buried interface, further from either surface. These signals can be seen for samples A and C in Figs. 4 and 6, respectively. Unfortunately the results from coil 2 in sample B were of very poor quality and have been omitted from Fig. 5 for clarity. One anomaly is that the signal from the upper part of coil 2 in sample C increases over the first few days, whereas the signal from coil 1 decreases. This is probably related to the single day of open cure leading up to the first measurement for sample C, when the topping was exposed to the atmosphere and the fact that sample C rapidly absorbs water from the base during the first few days. However, there is insufficient information to perform a detailed mass balance.

5. Conclusions

In this paper the NMR-MOUSE has been demonstrated as a viable device for assessing water content below the surface of concrete, although in this study it appeared to lack the ability to distinguish water in the different pore structures. Being a portable, hand-held device, the MOUSE may be of use on a construction project to determine when a concrete slab has dried sufficiently to apply a topping or second concrete pour without the risk of critical failure due to evaporable water collecting at the interface. A method for studying water transport across such an interface has been demonstrated that used embedded coils in a stray magnetic field to determine the water saturation at various depths throughout the sample. Although the susceptibility gradients caused by aggregates within the concrete mixes prevented the measurement of spatially resolved profiles, the integrated signal intensities correlated well with the estimated water content. Overall the results provided time-dependent measurements of the water fractions within the two layers. With further work, this system may provide a means of studying permeability and water transport through any materials into which a coil can be embedded.

Acknowledgements

JB would like to thank the British Council for funding scientific exchange between the Institute of Molecular Physics, Poznan, Poland, and the University of Surrey, UK. JM would like to thank the Royal Society for financial support. Finally we would also like to thank Professor John Strange for the use of NMR-MOUSE at the University of Kent, UK.

References

[1] R. Littlewood, Floor Coatings and Screeds: Living with Stresses. Engineering Briefing Document, (Reprinted from a paper given in Flooring Magazine, 2000), Flooring Associates, Chesterfield, 2001.

[2] A.J. Bohris, U. Goerke, P.J. McDonald, M. Mulheron, B. Newling, B.L. Page, A broad line NMR and MRI study of water and water transport in Portland cement pastes, Magn. Reson. Imaging 16 (5/6) (1998) 455–461.

[3] T. Nunes, E.W. Randall, A.A. Samoilenkoi, P. Bodart, G. Feio, The hardening of Portland cement studied by 1H NMR stray-field imaging, J. Phys., D, Appl. Phys. 29 (1996) 805–808.

[4] W.P. Halperin, J.-Y. Jehng, Y.-Q. Song, Application of spin–spin relaxation to measurement of surface area and pore size distributions in a hydrating cement paste, Magn. Reson. Imaging 12 (2) (1994).

[5] J.-Y. Jehng, D.T. Sprague, W.P. Halperin, Pore structure of hydrating cement paste by magnetic relaxation analysis and freezing, Magn. Reson. Imaging 14 (7/8) (1996) 785–791.

[6] J. Greener, H. Peemoeller, C. Choi, R. Holly, E.J. Reardon, C.M. Hansson, M.M. Pintar, Monitoring of hydration of white cement paste with proton NMR spin–spin relaxation, J. Am. Ceram. Soc. 83 (3) (2000) 623–627.

[7] D.D. Lasic, J.M. Corbett, J. Jian, J.C. MacTavish, M.M. Pintar, R. Blinc, G. Lahajnar, NMR spin grouping in hydrating cement at 200 MHz, Cem. Concr. Res. 18 (1988) 649–653.
[8] NMR-MOUSE is a registered trade mark of RWTH-Aachen, Germany.
[9] G. Eidmann, R. Savelsberg, P. Blümler, B. Blümich, The NMR MOUSE, a mobile universal surface explorer, J. Magn. Reson., Ser. A 122 (1996) 104–109.
[10] S. Sharma, F. Casanova, W. Wache, A. Segre, B. Blümich, Analysis of historical porous building materials by the NMR-MOUSE(R), Magn. Reson. Imaging 21 (3/4) (2003) 249–255.
[11] Premixed gypsum final coat plaster, Types b.1 and b.2, part 1, CLASS B, BS:1191.
[12] Ordinary Portland Cement, OPC, Type I, BS:12, 1989.
[13] Resonance Instruments Ltd. 31a Avenue One, Witney, Oxfordshire OX28 4XZ, UK.
[14] G.A. Matzkanin, C.G. Gardner, Nuclear magnetic resonance sensors for moisture measurement in roadways, Trans. Res. Rev. 532 (1975) 77–86.
[15] R.J.S. Brown, I. Fatt, Measurements of fractional wettability of oilfield rocks by the nuclear magnetic relaxation method, Pet. Trans. 207 (1956) 262–264.
[16] R.J.S. Brown, G.C. Borgia, P. Fantazzini, E. Mesini, Problems in identifying multimodal distributions of relaxation times for NMR in porous media, Magn. Reson. Imaging 9 (1991) 687–693.
[17] R.G. Palmer, D.L. Stein, E. Abrahams, P.W. Anderse, Models of hierarchically constrained dynamics for glassy relaxation, Phys. Rev. Lett. 53 (1984) 958–961.
[18] J.R. Zimmerman, W.E. Brittin, NMR studies in multiple phase systems: lifetime of a water molecule in an adsorbing phase on silica gel, J. Phys. Chem. 61 (1957) 1328–1333.
[19] F. D'Orazio, S. Bhattacharja, W.P. Halperin, Molecular diffusion and NMR relaxation of water in unsaturated porous silica glass, Phys. Rev., B 42 (16) (1990) 9810–9818.
[20] J. Mitchell, S.C. Stark, J.H. Strange, Probing surface interactions by combining NMR cryoporometry and NMR relaxometry, J. Phys., D, Appl. Phys. 38 (2005) 1950–1958.
[21] C. Choi, J. Peternlj, M.M. Pintar, A method for measuring the diffusivity of a liquid into a porous matrix, J. Chem. Phys. 109 (5) (1998) 1860–1862.
[22] A.M. Neville, Properties of Concrete, Longman Scientific & Technical, Singapore, 1991.